

Achieving Low-Latency Mobile Edge Computing by Uplink and Downlink Decoupled Access in HetNets

Ali Al-Shuwaili and Ahmed Lawey

Abstract—Despite the physical proximity of computationally-enhanced Base Stations (BSs) in Mobile Edge Computing (MEC) systems, achieving an end-to-end low-latency for computations offloading is still a critical design problem. This is because the offloading of computational tasks via the MEC or cloudlet servers entails the use of uplink and downlink radio links that are usually assumed to be coupled to a single BS. However, for heterogeneous networks, a new architectural paradigm whereby uplink and downlink are not associated with the same BS is proposed and seen to provide gains in network throughput. Motivated by such gains, and by using typical results from stochastic geometry, we formulate the offloading latency for the MEC-based scheme with decoupled UL/DL association, or decoupled access, and compare its performance to the conventional coupled or single association scheme. Despite the extra backhaul delay necessary for the communication between the two serving BSs in UL and DL, the MEC-based offloading scheme with decoupled association is still capable of providing a fairly lower offloading latency as compared to the conventional offloading scheme with coupled association.

Index Terms—Mobile edge computing, Decoupled access, Offloading, Latency, Backhaul

I. INTRODUCTION

Leveraging the computational capabilities of the nearby Base Stations (BSs), known as Mobile Edge Computing (MEC), seems to be unavoidable technique to cope with the computing and battery capacity limitations of mobile devices [1]. Due to the variability of the UL/DL communication network through which the edge computing server, or cloudlet, is accessed, unpredictable energy expenditure or intolerable delay might be experienced during the communications between Mobile Users (MUs) and cloudlet servers. Given that offloading requires transmission and reception on the wireless interface in UL and DL respectively, many recent lines of work have demonstrated that it is possible to design an energy- and latency-efficient mobile edge computing systems by, for example, performing a joint optimization of the UL/DL allocation of communication and computational resources [2].

To meet the stringent latency requirements for delay-sensitive applications like medical or AR/VR applications, feasible offloading time needs to be in order of milliseconds [2]. Such critical latency values are potentially limited by the type of MU-BS association employed by the network and by the number of offloading users as these two factors

A. Al-Shuwaili is with the Center for Wireless Information Processing (CWiP), Department of Electrical and Computer Engineering, New Jersey Institute of Technology, Newark, NJ 07102 USA (e-mail: ana24@njit.edu).

A. Lawey is with the School of Electronic and Electrical Engineering, University of Leeds, United Kingdom (e-mail: a.q.lawey}@leeds.ac.uk).

determine the resulting interference level in UL and DL in addition to resource utilization. For instance, if too many MUs simultaneously choose to offload their computational tasks, the resulting interference on the wireless channel may violate the feasibility of offloading by requiring an energy consumption at the mobile for wireless transmission that exceeds the energy that would be needed for local computing or result in an offloading latency higher than the application’s deadline.

The typical structure of current wireless networks constraints users to associate to the same BS in both uplink and downlink. In DL, the MUs first associate to the BS that provide the highest average power, and then use the same BS for UL transmission [3], [4]. This *coupled* association scheme is efficient for traditional cellular network where single type of BSs are regularly deployed and have identical radio capabilities. However, with the emergence of heterogeneous networks where different types of BSs, like macro, femto or pico, are coexisted in multi-tier set-up, the coupled association scheme requires further consideration.

Departing from this traditional coupled access, an emerging paradigm in 5G systems that is shown to improve the capacity of such heterogeneous networks is by treating uplink and downlink as separate network connections [3], [4]. As previously stated, in MEC-based systems, the feasibility of computational tasks offloading is potentially limited by the type of MU-BS association policy employed in the network. Therefore, in this paper, we propose an MEC-based offloading scheme that applies different association policies for uplink and downlink, i.e., with *decoupled* association, and analyze its performance, in terms of the offloading latency, using stochastic geometry tools. Section II introduces the system model and also the formulation of the offloading latency expressions while numerical results are provided in Section III. Concluding remarks are finally provided in Section IV.

II. SYSTEM MODEL

A heterogeneous mobile edge computing network that consists of a two-tier deployment of Macro cell Base Stations (MBSs) and Small cell Base Stations (SBSs) is considered. Both tiers operate on the same frequency band and using Frequency Division Duplex (FDD) [3]. The locations of BSs in the k th tier, with $k \in \{M, S\}$, are modeled according to a two-dimensional homogeneous Poisson Point Process (PPP) Φ_k with density λ_k . The transmission powers of all BSs in the same tier are assumed to be identical and are denoted as P_k with $k \in \{M, S\}$. The locations of the MUs in the network are also modeled according to a homogeneous PPP

Φ_u with density λ_u that is independent of the BS locations Φ_M and Φ_S . We also assume that the MUs in the same BS use an OFDMA-like orthogonal multiple access scheme, such that there is exactly one user per cell that is scheduled on the same time-frequency resource each with transmit power of P_u . Signals in both uplink and downlink are assumed to experience path loss with path loss exponent $\alpha > 2$. Each receiver has a constant noise power of σ^2 .

A local computing server, or ‘‘cloudlet’’, is directly connected to each BS in both tiers (see Fig. 1). We generally assume that the MBSs’ cloudlets have a higher computation capacity as compared to the SBSs’ cloudlets [1]. Denoting as F_k the cloudlet computation capacity in CPU cycles per seconds for the BSs in tier k , we then have $F_M \geq F_S$. Also, a SBS is connected to the closest MBS via a finite capacity backhaul link. The capacity in bits per seconds of the backhaul link that connects an SBS to an MBS is denoted as C^{bh} .

MU-BS association policy can be either coupled or decoupled. With the conventional coupled access, each MU is assigned in both UpLink (UL) and DownLink (DL) to the BS that offers maximal received power in the DL. Instead, with decoupled access, the MU is associated in the DL to the BS from which it receives the maximal power while, for the UL, it is associated to the BS that receives its signal with the highest average power [4], [5].

Each MU wishes to run an application that is characterized by the number V of CPU cycles necessary to complete one request from that application, by the number B^I of input bits necessary to offload the computations of one request to the cloudlet processor, and by the number B^O of output bits encoding the result of the computation (see, e.g., [2]). To offload an application, the MU first transmits the B^I input bits to its associated MBS or SBS; then a cloudlet executes the V CPU cycles; and finally the B^O output bits are sent back to the MU. As it will be discussed, the execution of the application can take place at the cloudlet attached to the BS to which the MU is connected in the UL or to the BS to which the MU is connected in the DL. As seen, the UL and DL BSs, in fact, need not to be the same in the presence of a decoupled access policy. Furthermore, in such cases, backhaul transmission is necessary for the communications between the the UL and DL BSs. The association model for both coupled and decoupled access is discussed next. Throughout, the analysis will assume the existance of the typical MU, i.e., an MU that is located at the origin [5], [6].

A. Association Model

Let $\|x_k^0\|$ be the distance from the typical MU to the nearest k BS with $k \in \{M, S\}$, we then formulate the association rule as

$$\underset{k \in \Phi_M \cup \Phi_S}{\operatorname{argmax}} T_k \|x_k^0\|^{-\alpha}, \quad (1)$$

where T_k is a parameter that specifies the access or association type in UL and DL as explained next.

(1) *Coupled access*: It is a DL-based association policy where, by setting $T_k = P_k$ with $k \in \{M, S\}$ in (1), the MU is

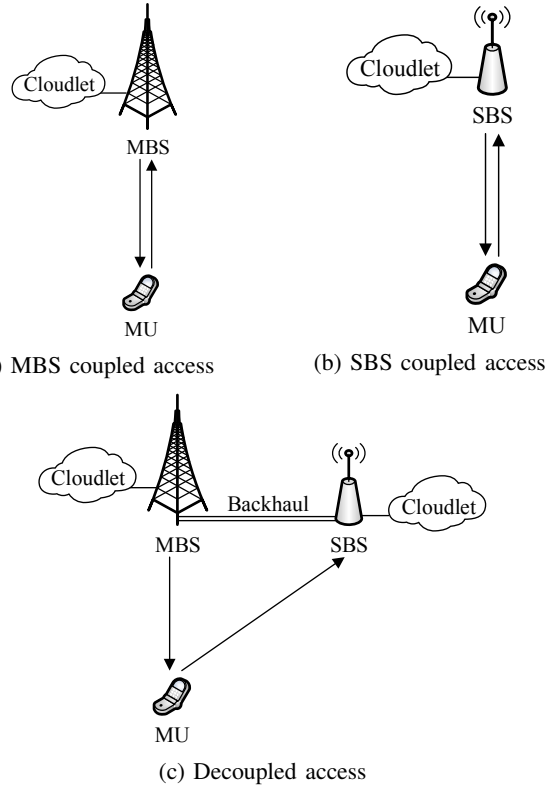


Fig. 1: System model: Mobile users (MUs) offload the execution of their applications to a cloudlet processor in two-tier heterogeneous networks: (a) Coupled access with MBSs in UL and DL; (b) Coupled access with SBSs in UL and DL; (c) Decoupled access with MBSs in the DL tier and SBSs in the UL tier. The latter case requires that a SBS to have a backhaul connection to the closest MBS. Note that coupled, or DL-based, association, implies (a) and (b) cases while decoupled, or UL-based, association, implies (a), (b) and (c) cases.

associated to the BS from which it receives the highest average power. The same BS will also be the serving BS for the uplink connection. As a result, with the two-tier heterogeneous network considered in this model, the coupled association can lead to two possible association cases: (i) Case 1: UL base station = DL base station = SBS and (ii) Case 2: UL base station = DL base station = MBS. We denote by A_{kl}^D the association probability when the MU is associated to a k BS in UL and a l BS in DL with $k = l \in \{M, S\}$ and the association is DL-based or coupled. The corresponding association probabilities for these two cases can be obtained from the general expression in [6, Lemma 1] as:

(i) *Case 1: UL base station = DL base station = SBS*:

$$A_{SS}^D = \frac{\lambda_S}{\lambda_S + (\frac{P_M}{P_S})^{2/\alpha} \lambda_M}; \quad (2)$$

(ii) *Case 2: UL base station = DL base station = MBS*:

$$A_{MM}^D = \frac{\lambda_M (\frac{P_M}{P_S})^{2/\alpha}}{\lambda_S + (\frac{P_M}{P_S})^{2/\alpha} \lambda_M}. \quad (3)$$

(2) *Decoupled access*: It is an UL-based association policy whereby, by setting $T_k = 1$ with $k \in \{M, S\}$ in (1), the MU is associated to the BS to which it transmits with the highest average power. The concept of decoupled access implies, based on (1), that MU can select two different base stations, each one corresponds to different network connection, i.e., UL and DL. For this case, the association process can lead to one of the four possible association cases: (i) Case 1: UL base station = DL base station = SBS; (ii) Case 2: UL base station = DL base station = MBS; (iii) Case 3: UL base station = SBS and DL base station = MBS; (iv) Case 4: UL base station = MBS and DL base station = SBS. We also denote by A_{kl}^U the association probability when the MU is associated to a k BS in UL and a l BS in DL with $k, l \in \{M, S\}$ and the association is UL-based or decoupled. Following the procedures in [5], the association probabilities for these cases are given as follows:

(i) *Case 1: UL base station = DL base station = SBS*:

$$A_{SS}^U = \frac{\lambda_S}{\lambda_S + (\frac{P_M}{P_S})^{2/\alpha} \lambda_M}; \quad (4)$$

(ii) *Case 2: UL base station = DL base station = MBS*:

$$A_{MM}^U = \frac{\lambda_M}{\lambda_M + \lambda_S}; \quad (5)$$

(iii) *Case 3: UL base station = SBS and DL base station = MBS*:

$$A_{SM}^U = \frac{\lambda_S}{\lambda_S + \lambda_M} - \frac{\lambda_S}{\lambda_S + (\frac{P_M}{P_S})^{2/\alpha} \lambda_M}; \quad (6)$$

(iv) *Case 4: UL base station = MBS and DL base station = SBS*:

$$A_{MS}^U = 0. \quad (7)$$

The total offloading latency depends on the type of association which will be discussed in Section II-D after formulating the communication and computation times for coupled and decoupled access in Section II-B and Section II-C, respectively.

B. Communication and Computation Model with Coupled Access

In this section, we derive the latency resulting from offloading the applications of the typical MUs. The offloading latency consists of the time L^{ul} needed for the MU to transmit the input bits to its serving BS in the uplink; the time L^{exe} necessary for the cloudlet to execute the instructions; the time L^{bh} for exchanging information between BSs in different tiers; and the time L^{dl} to send the result back to the MU in the downlink (see Fig. 1). We can hence write the total offloading latency for a typical MU with decoupled access as

$$L = L^{ul} + L^{exe} + L^{bh} + L^{dl}. \quad (8)$$

It is noted here that the offloading latency for the coupled access scheme is a special case of (8) which is obtained with $L^{bh} = 0$. In the rest of this section, we derive an expression for each latency term in (8) under coupled association. The latency analysis for decoupled association is deferred to Section II-C.

1) *Uplink transmission*: The average rate, in bits/s, for transmitting the input bits of a typical MU in the uplink using DL-based or coupled association is given by

$$R_{D,k}^{ul}(\gamma_k^{ul}) = \frac{W^{ul}}{N_{D,k}} \log_2(1 + \gamma_k^{ul}) P_{D,k}^{ul}(\gamma_k^{ul}), \quad (9)$$

where γ_k^{ul} is the target SINR threshold for MU connected to the k th tier in the uplink; W^{ul} is the uplink bandwidth in Hz; $N_{D,k}$ is the average number of uplink MUs associated with a BS in the k th tier using DL-based association and is given by $N_{D,k} = \lambda_u A_{kl}^D / \lambda_k$ where A_{kl}^D is the association probability as given in (2) and (3) with $k = l = S$ for SBS tier and $k = l = M$ for MBS tier, respectively; and $P_{D,k}^{ul}(\gamma_k^{ul})$ is the coverage probability in the uplink of heterogeneous network, i.e., the probability that the instantaneous uplink SINR is larger than or equal to the corresponding thresholds γ_k^{ul} when a typical MU is associated with k th tier via DL-based or coupled association. Throughout, for notation simplicity, we consider identical per-tier SINR thresholds, i.e., $\gamma_k^{ul} = \gamma^{ul}$ for all k . This probability is derived in [5] as

$$P_{D,k}^{ul}(\gamma^{ul}) = \int_0^\infty e^{-\frac{\gamma^{ul} \sigma^2 x^\alpha}{P_u}} e^{-\pi \tilde{\lambda}_u \psi(\gamma^{ul}, \alpha) x^2} f_{X_k}^D(x) dx, \quad (10)$$

where $\tilde{\lambda}_u = p \lambda_u$ with p being the thinning probability given by $p = (\lambda_M + \lambda_S) / \lambda_u$ and $f_{X_k}^D(x)$ is the Probability Density Function (PDF) of the distance between a typical MU and its serving BS using DL-based association which reads [5]

$$f_{X_k}^D(x) = \frac{2\pi \lambda_k}{A_{kl}^D} x e^{-\left(\lambda_k + \lambda_j \left(\frac{P_j}{P_k}\right)^{(2/\alpha)}\right) \pi x^2} \quad (11)$$

and, for $\alpha = 4$, $\psi(\gamma^{ul}, \alpha) = \sqrt{\gamma^{ul}} \arctan \sqrt{\gamma^{ul}}$ [6]. The time, in seconds, necessary to complete the uplink transmissions to the k th tier in coupled access is defined as

$$L_{D,k}^{ul}(\gamma^{ul}) = \frac{B^I}{R_{D,k}^{ul}(\gamma^{ul})}. \quad (12)$$

2) *Downlink transmission*: The downlink rate function, in bits/s, depends on the target SINR threshold level in the downlink γ_k^{dl} according to the relation

$$R_{D,k}^{dl}(\gamma_k^{dl}) = \frac{W^{dl}}{N_{D,k}} \log_2(1 + \gamma_k^{dl}) P_{D,k}^{dl}(\gamma_k^{dl}), \quad (13)$$

with W^{dl} being the downlink bandwidth and $P_{D,k}^{dl}(\gamma_k^{dl})$ is the probability of coverage in the downlink, i.e., the probability that the instantaneous SINR is larger than or equal to the corresponding thresholds γ_k^{dl} for a typical MU in the DL. Assuming identical per-tier SIR thresholds ($\gamma_k^{dl} = \gamma^{dl}$ for all k), the DL coverage probability is derived in [7] as

$$P_{D,k}^{dl}(\gamma^{dl}) = \int_0^\infty e^{-\frac{\gamma^{dl} \sigma^2 x^\alpha}{P_k} (1 + \psi(\gamma^{dl}, \alpha))} f_{X_k}^D(x) dx, \quad (14)$$

with $\psi(\gamma^{dl}, 4) = \sqrt{\gamma^{dl}} \arctan \sqrt{\gamma^{dl}}$. The time, in seconds, necessary to complete the downlink transmission from the k th tier in coupled access is

$$L_{D,k}^{dl}(\gamma^{dl}) = \frac{B^O}{R_{D,k}^{dl}(\gamma^{dl})}. \quad (15)$$

3) *Edge processing:* The computation servers in both tiers are assumed to have $M/M/1$ queuing system. With this model, the requests arrive according to a Poisson process with rate τ requests per second. The service rate are also assumed to be independent and exponentially distributed with parameter μ requests per seconds. It is well known from queuing theory that the mean request delay of such servers is given by $1/(\mu - \tau)$. Motivated by this formula, we will derive a general expression for the computation time that captures both the tier in which the executions are performed and the load, in terms of the average number of associated users, of the serving BS as discussed next.

Let us first write the service rate μ_k in tier k as

$$\mu_k = \frac{F_k}{V}, \quad (16)$$

where $k = M$ for MBS and $k = S$ for SBS. It is noted here that the service rate is depending on the computation capability of the BS in tier k that process the offloaded tasks. As mentioned in Section I, we realistically require $F_M \geq F_S$.

Next, to calculate the request arrival rate τ_k in tier k , we define d_k as the accumulated uplink rates for all the MUs that are connected to the same BS in tier k . We can then write

$$\tau_k = \frac{d_k}{B^I}, \quad (17)$$

with $k \in \{M, S\}$. To find an expression for d_k , we first observe that d_k is depending on the number of MUs that are served by the k th BS in the uplink. For a Voronoi cell, it is proved in [8] that the average area of a Voronoi cell in tier k is $1/\lambda_k$. We then have the average number of served MUs as $(\lambda_u/\lambda_k)A_{kl}^D = N_{D,k}$ for $k \in \{M, S\}$. Building on these formulations, we can rewrite d_k as

$$d_k = R_{D,k}^{ul}(\gamma^{ul}) \frac{\lambda_u}{\lambda_k} A_{kl}^D. \quad (18)$$

Combining (16), (17) and (18), we can have the general expression for the edge processing time at k th tier with coupled access as

$$L_{D,k}^{\text{exe}} = \frac{1}{\frac{F_k}{V} - \frac{R_{D,k}^{ul}(\gamma^{ul})}{B^I} N_{D,k}}, \quad (19)$$

where $k = M$ for MBS and $k = S$ for SBS. Clearly, $\mu_k > \tau_k$ is required for the stability of (19).

C. Communication and Computation Model with Decoupled Access

In a manner similar to the previous section, we formulate here the uplink, execution and downlink times for decoupled association as detailed next.

1) *Uplink transmission:* Similar to (9), the average uplink rate of a typical MU associated with k th tier using UL-based, or decoupled, association is given by

$$R_{U,k}^{ul}(\gamma^{ul}) = \frac{W^{ul}}{N_{U,k}^{ul}} \log_2(1 + \gamma^{ul}) P_{U,k}^{ul}(\gamma^{ul}), \quad (20)$$

where $N_{U,k}^{ul} = \lambda_u A_k^{ul} / \lambda_k$ is the average number of associated MUs to a BS in the k th tier for the UL connection with A_k^{ul} being the association probability for the k th tier BS in UL which depends on the association probabilities (4)-(7) according to the relation $A_k^{ul} = \sum_{l \in \{M, S\}} A_{kl}^U$. For instance, the probability that MU is connected to SBS tier in UL with decoupled access association is simply $A_S^{ul} = A_{SS}^U + A_{SM}^U$, where A_{SS}^U and A_{SM}^U are given in (4) and (6), respectively. The coverage probability for this case is given by [5]

$$P_{U,k}^{ul}(\gamma^{ul}) = \int_0^\infty e^{-\frac{\gamma^{ul} \sigma^2 x^\alpha}{P_u}} e^{-\pi \tilde{\lambda}_u \psi(\gamma^{ul}, \alpha) x^2} f_{X_k}^U(x) dx, \quad (21)$$

with $f_{X_k}^U(x)$ is the PDF of the distance between a typical MU and its serving BS for UL-based association which reads [5]

$$f_{X_k}^U(x) = \frac{2\pi\lambda_k}{A_k^{ul}} x e^{-(\lambda_k + \lambda_j)\pi x^2}. \quad (22)$$

The decoupled-enabled transmission time in uplink is then given by

$$L_{U,k}^{ul}(\gamma^{ul}) = \frac{B^I}{R_{U,k}^{ul}(\gamma^{ul})}. \quad (23)$$

2) *Downlink transmission:* Similar to the uplink, we can write the average rate in bits per seconds for the typical MU associated to the l th tier in the downlink using UL-based association as

$$R_{U,l}^{dl}(\gamma^{dl}) = \frac{W^{dl}}{N_{U,l}^{dl}} \log_2(1 + \gamma^{dl}) P_{U,l}^{dl}(\gamma^{dl}), \quad (24)$$

where $N_{U,l}^{dl} = \lambda_u A_l^{dl} / \lambda_l$ is the average number of associated MUs to a BS in the l th tier for the DL connection with decoupled access and A_l^{dl} being the association probability for the l th tier BS in DL which depends on the association probabilities (4)-(7) according to the relation $A_l^{dl} = \sum_{k \in \{M, S\}} A_{kl}^U$. For instance, the probability that MU is connected to SBS tier in DL with decoupled access association is simply $A_S^{dl} = A_{SS}^U + A_{MS}^U$, where A_{SS}^U and A_{MS}^U are given in (4) and (7), respectively. The coverage probability $P_{U,l}^{dl}(\gamma^{dl})$ is obtained from (14) after substituting A_{kl}^D by A_l^{dl} . The corresponding required transmission time in DL with UL-based association reads

$$L_{U,l}^{dl}(\gamma^{dl}) = \frac{B^O}{R_{U,l}^{dl}(\gamma^{dl})}. \quad (25)$$

3) *Edge processing:* With UL-based association, when the MU is connected to different BSs in UL and DL, the offloaded application can be processed at either one of the associated BSs. Accordingly, we distinguish the following two decoupled cases.

(i) *UL Cloudlet processing time:* The time needed to process the offloaded task at the uplink cloudlet or k th tier BS is written as

$$L_{U,k}^{\text{exe}} = \frac{1}{\frac{F_k}{V} - \frac{R_{U,k}^{ul}(\gamma^{ul})}{B^I} N_{U,k}^{ul}}. \quad (26)$$

We emphasize here that the expression in (26) is used to calculate the execution time for any association case that can result from decoupled access, i.e., $k = M$ and $k = S$ in UL, since in both cases the processing takes place at UL cloudlet. Therefore, it is natural for (26) to have similar expression to the coupled access execution time in (19). This is a direct result from the fact that decoupling the DL transmission from UL has no effect on the processing time when computations are performed at the BS to which MU are connected in UL. However, with DL cloudlet processing, the execution time need more careful consideration as discussed next.

(ii) *DL Cloudlet processing time*: If the processing takes place at the downlink cloudlet or l th tier BS, the execution time is given by

$$L_{U,l}^{\text{exe}} = \frac{1}{\frac{F_l}{V} - \left(\frac{R_{U,l}^{\text{ul}}(\gamma^{\text{ul}})}{B^I} N_{U,l}^{\text{ul}} + \frac{R_{U,k}^{\text{ul}}(\gamma^{\text{ul}})}{B^I} \frac{\lambda_u}{\lambda_k} A_{SM}^U \right)}. \quad (27)$$

Unlike (26), the above expression applies specifically to determine the execution time only when $l = M$. This is because with DL cloudlet processing, the MBS, or downlink, cloudlet receives requests from both the $N_{U,l}^{\text{ul}}$ fraction of MUs that are associated to MBS in UL and also the requests from A_{SM}^U fraction of MUs that are transferred to DL cloudlet via backhaul links. For $l = S$, since the requests arrive to UL cloudlet via the UL connections only from A_{SS}^U fraction of MUs, therefore the execution time reads

$$L_{U,l}^{\text{exe}} = \frac{1}{\frac{F_l}{V} - \frac{R_{U,k}^{\text{ul}}(\gamma^{\text{ul}})}{B^I} \frac{\lambda_u}{\lambda_k} A_{SS}^U}. \quad (28)$$

D. Offloading Latency

In order to compare the latency performance resulting from the offloading under coupled and decoupled access, we next formulate the overall offloading latency experienced by the typical MU for both association types. We conclude this section by presenting the average offloading latency.

1) *Offloading latency with coupled access*: The offloading latency for the typical MU associated to a given SBS or MBS, in both UL and DL, is

$$L_{kl}^D(\gamma^{\text{ul}}, \gamma^{\text{dl}}) = L_{D,k}^{\text{ul}}(\gamma^{\text{ul}}) + L_{D,k}^{\text{exe}} + L_{D,k}^{\text{dl}}(\gamma^{\text{dl}}), \quad (29)$$

where $k = l = M$ for MBS and $k = l = S$ for SBS.

When the MU is connected to different BSs in UL and DL, the offloaded application can be processed at either one of the associated BSs. Accordingly, we distinguish the following two decoupled cases.

2) *Offloading latency with decoupled access and UL cloudlet processing*: When the user is associated to a k BS in UL and a l BS in DL with $k, l \in \{M, S\}$ and processing takes place at the cloudlet of the k BS, the overall offloading latency experienced by the MU is then given by

$$\dot{L}_{kl}^U(\gamma^{\text{ul}}, \gamma^{\text{dl}}) = L_{U,k}^{\text{ul}}(\gamma^{\text{ul}}) + L_{U,k}^{\text{exe}} + L_k^{\text{bh}} + L_{U,l}^{\text{dl}}(\gamma^{\text{dl}}). \quad (30)$$

Note that, in this case, the backhaul is used to transfer the output bits produced by the execution at the k BS with corresponding transmission delay of $L_k^{\text{bh}} = B^O/C^{\text{bh}}$.

3) *Offloading latency with decoupled access and DL cloudlet processing*: When the user is associated to a k BS in UL and a l BS in DL with $k, l \in \{M, S\}$ and processing takes place at the cloudlet of the l BS, the offloading latency is

$$\dot{L}_{kl}^U(\gamma^{\text{ul}}, \gamma^{\text{dl}}) = L_{U,k}^{\text{ul}}(\gamma^{\text{ul}}) + L_l^{\text{bh}} + L_{U,l}^{\text{exe}} + L_{U,l}^{\text{dl}}(\gamma^{\text{dl}}). \quad (31)$$

In this case, the backhaul carries the input bits that are to be processed by the l BS with communication time given by $L_l^{\text{bh}} = B^I/C^{\text{bh}}$.

4) *Average Offloading Latency*: Given the association probabilities in Section II-A and the offloading latency in (29)-(31), the average offloading latency for coupled access can be then given by

$$L^D(\gamma^{\text{ul}}, \gamma^{\text{dl}}) = \sum_{k \in \{M, S\}} A_{kl}^D L_{kl}^D(\gamma^{\text{ul}}, \gamma^{\text{dl}}). \quad (32)$$

with $l = k$. For the decoupled access with UL cloudlet processing we write

$$\dot{L}^U(\gamma^{\text{ul}}, \gamma^{\text{dl}}) = \sum_{k \in \{M, S\}} \sum_{l \in \{M, S\}} A_{kl}^U \dot{L}_{kl}^U(\gamma^{\text{ul}}, \gamma^{\text{dl}}), \quad (33)$$

and similarly for DL cloudlet processing we have

$$\dot{L}^U(\gamma^{\text{ul}}, \gamma^{\text{dl}}) = \sum_{k \in \{M, S\}} \sum_{l \in \{M, S\}} A_{kl}^U \dot{L}_{kl}^U(\gamma^{\text{ul}}, \gamma^{\text{dl}}). \quad (34)$$

III. NUMERICAL RESULTS

In this section, we present numerical results with the main aims of comparing the latency performance of the proposed offloading scheme in which decoupled association is adopted with the more conventional scheme whereby uplink and downlink connections are always associated with the same BS. To this end, we consider a two-tier setting with the macro tier described by $\lambda_M = 1$ BS per sq. km, $P_M = 46$ dBm [5], [7] and $F_M = 4.5$ GHz [9], while the tier of SBSs is characterized by $\lambda_S = 10$ BS per sq. km, $P_S = 30$ dBm [5], [7] and $F_S = 3.6$ GHz [10]. The user density is $\lambda_u = 25$ MU per sq. km with $P_u = 20$ dBm [5]. The uplink and downlink bandwidth is $W^{\text{ul}} = W^{\text{dl}} = 1.4$ MHz [11] and also we set $\sigma^2 = -120$ dBm with $\alpha = 4$. We select $B^I = 4B^O$ with $B^O = 1$ kbits and the required CPU cycles of the offloaded components is set to $V = 2640 \times B^I$ CPU cycles [12]. Unless otherwise stated, we select the backhaul capacity as $C^{\text{bh}} = 10$ Mbits/s [2] and $\gamma^{\text{ul}} = \gamma^{\text{dl}} = -10$ dB.

We first compare the latency performance of the both coupled and decoupled association schemes discussed in Section II-D. To this end, Fig. 2 plots the offloading latency for the coupled access scheme in (32), marked as “Coupled Access” in Fig. 2, against the SINR thresholds in UL and DL which are assumed to be identical, i.e., $\gamma^{\text{ul}} = \gamma^{\text{dl}}$. Shown in the same figure, is the latency performance for decoupled access scheme given in (33) and (34) for UL and DL cloudlet

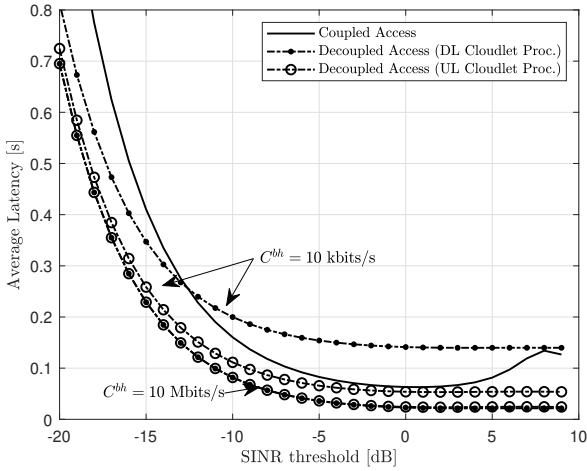


Fig. 2: Average mobile offloading latency for coupled and decoupled access offloading schemes in (32)-(34) versus the target SINR threshold value $\gamma^{ul} = \gamma^{dl}$.

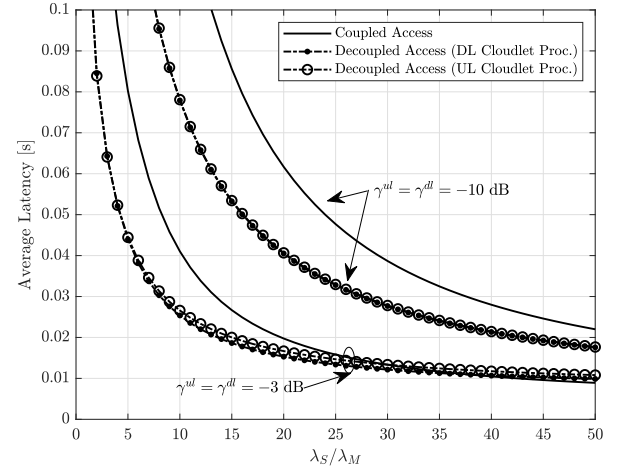


Fig. 3: Average mobile offloading latency for coupled and decoupled access offloading schemes in (32)-(34) as a function of the BSs density ratio λ_S/λ_M .

processing, which are marked as “Decoupled Access (UL Cloudlet Proc.)” and “Decoupled Access (DL Cloudlet Proc.)”, respectively. The key observation here is that the performance of the decoupled access is strongly limited by the backhaul capacity. For instance, with backhaul $C^{bh} = 10$ kbit/s, it is observed that the decoupled access scheme with DL processing requires an offloading latency that is 25% higher than the coupled access scheme at $\gamma^{ul} = \gamma^{dl} = -10$ dB. However, with backhaul 10 Mbit/s the decoupled access scheme starts to have a noticeably lower offloading latency. At SINR $\gamma^{ul} = \gamma^{dl} = -15$ dB, for example, the decoupled access scheme attains 42% latency reduction as compared to the coupled access scheme. The reason for this improvement, with the improved backhaul connections between the two tiers, is the fact that the decoupled access scheme requires a certain fraction of MUs to decouple their associations between the two tiers, i.e., $k = S$ and $l = M$ for A_{SM}^U percentage of users since $A_{MS}^U = 0$. This decoupling in UL/DL association brings two improvements to the performance of the decoupled scheme: first, an improved UL time for the A_{SM}^U fraction of MUs due to the physical proximity, and hence better UL coverage, and also the higher density of SBSs tier compared to the tier of MBSs which implies more availability of radio resources, e.g., uplink bandwidth. Second, as a result of the first point, for the fraction of MUs which remain in coupled access to MBSs with UL-based association, i.e., A_{MM}^U , will now benefit from both the more availability of resources and the enhanced coverage since the number of MUs coupled to MBS in UL is decreased after decoupling the association of some MUs, and hence an improvement in the uplink connection. These two gains combine to yield the latency saving of the proposed decoupled-based offloading scheme with respect to the conventional coupled offloading. We conclude from Fig. 2 that decoupling the UL/DL association, as more MUs select SBSs tier for

uplink transmission with decoupled access, will increase the competition among SBSs’ users over the limited available resources and increase the interference level. However, this is effectively alleviated with the higher density of SBSs tier and consequently an improved UL coverage. Finally, it is important to point out that that the limitation in backhaul capacity deteriorates the performance of the decoupled access scheme with DL processing due to the backhaul delay required to deliver B^I bits from SBS to MBS tiers. This backhaul delay has marginal impact on the performance of the decoupled access with UL processing scheme due to the reduced number of B^O bits transferred between the two tiers in this case. For higher backhaul capacity, e.g., $C^{bh} = 10$ Mbit/s, the backhaul time diminishes and thus the UL and DL processing cases for decoupled access scheme have similar offloading latency which is smaller than that required by coupled access scheme due to the aforementioned reduction in uplink time.

To obtain further insights, Fig. 3 shows the average per-MU offloading latency as a function of the ratio λ_S/λ_M that obtained by setting $\lambda_M = 1$ BS per sq. km and vary SBSs density λ_S . It is seen that for moderate density of BSs ($\lambda_S/\lambda_M < 25$), the decoupled access scheme provides significant savings in latency performance compared to coupled access as seen with 33% at $\gamma^{ul} = \gamma^{dl} = -3$ dB and with 43% at $\gamma^{ul} = \gamma^{dl} = -10$ dB for $\lambda_S = 15\lambda_M$. The saving can be attributed to the fact that, as the density of SBSs increases, more MUs favor the decoupled association and equivalently increase the probability A_{SM}^U or the fraction of MUs with uplink connection to SBSs and downlink connections to MBSs. Not surprisingly, as the SBSs become more *densified*, the probability of decoupled association diminishes resulting in comparable performance of both coupled and decoupled access schemes since $A_{SS}^D \approx A_{SS}^U \approx 1$ meaning that the majority of MUs have favored the SBSs tier for both uplink and downlink transmissions.

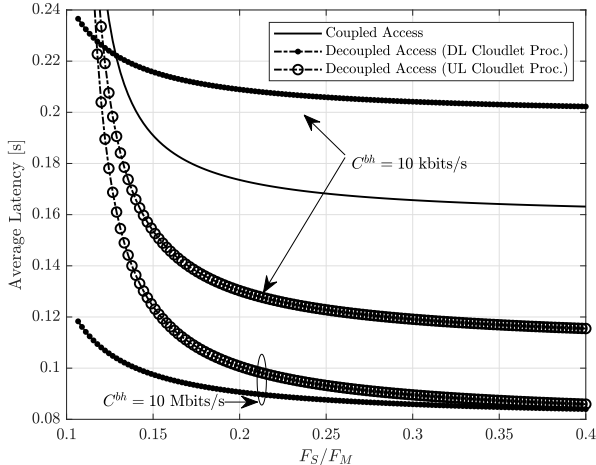


Fig. 4: Average mobile offloading latency for coupled and decoupled access offloading schemes in (32)-(34) as a function of the BSs computation capacity ratio F_S/F_M .

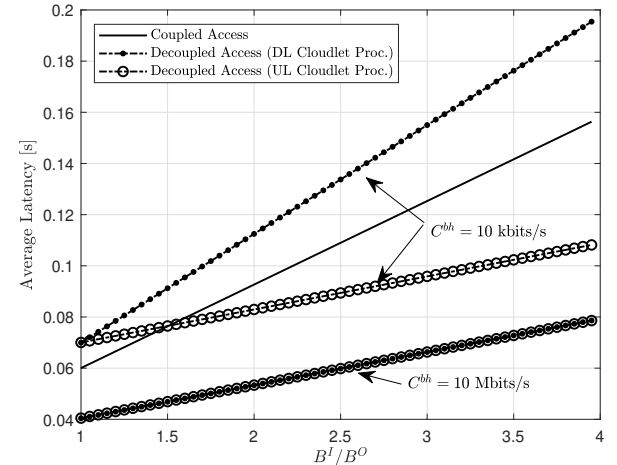


Fig. 5: Average mobile offloading latency for coupled and decoupled access offloading schemes in (32)-(34) versus the input-to-output bits ratio B^I/B^O .

We now turn to the role of the MEC capacity on the offloading latency under coupled and decoupled access schemes. In Fig. 4, we plot the average offloading latency as a function of the ratio of MEC servers computational capacity in the two tiers, or UL and DL cloudlets, denoted as F_S/F_M . It is observed that, when the backhaul capacity is limited, decoupling the UL/DL association is not advantageous in terms of offloading latency especially when utilizing the computational capability of the DL cloudlet. With UL cloudlet processing, since the saving of more computationally-capable MBSs is compensated by smaller backhaul transmission time when SBSs process the data due to $B^I = 4B^O$, the UL, or SBS, cloudlet is able to provide much lower execution time compared to DL cloudlet. As the backhaul capacity is increased, i.e. at $C^{bh} = 10$ Mbit/s, a considerable reduction in latency is achieved due to the improved connection between the two tiers as well as the saving in the UL transmission time with decoupled access as discussed in Fig. 2. This reduction is more pronounced with DL, or MBS, cloudlet since $F_M > F_S$ which compensates for the delay in backhaul links yielding an offloading latency lower than that required by coupled access scheme. For instance, with $F_S = 0.15F_M$, the decoupled access with DL cloudlet processing provides 55% reduction in latency compared to the coupled access scheme. It is worth to mention that the impact of decreasing the SBS computational capacity is more sever on the performance of the decoupled access with UL cloudlet processing. This is due to the higher arrival rate on the SBS cloudlet for the UL cloudlet processing case of the decoupled access scheme compared to the case of the DL cloudlet processing (cf. (26), (28)).

Finally, to highlight the impact of asymmetries in the offloading requirements, we plot in Fig. 5 the average offloading latency versus the ratio of input to output bits denoted as B^I/B^O which is obtained by setting $B^O = 1$ kbit and vary

B^I . When the offloaded applications have identical set of data in UL and DL, i.e., $B^I = B^O$, it is evident that processing the tasks at UL or DL cloudlets under decoupled access yields similar offloading latency, which is higher than that brought by coupled access scheme due to backhaul limitations at $C^{bh} = 10$ kbit/s. For $B^I/B^O > 1$, the UL cloudlet benefits from the reduced number of output data transferred over the backhaul connections which results in lower latency compared to both the coupled scheme and the decoupled access scheme with DL cloudlet processing. Moreover, with $C^{bh} = 10$ Mbit/s, the decoupled access scheme attains a latency reduction of 42% compared to the decoupled access scheme even at $B^I = B^O$.

IV. CONCLUDING REMARKS

The offloading of mobile computations with independent association of the uplink and downlink transmissions is investigated by merging computation offloading decision and the MU-BS association into a single system perspective. The offloading scheme with decoupled association yields considerable reduction in the total offloading latency. This saving is more pronounced in moderately densified networks and with fair backhaul connections where, in our results, it leads to a reduction of up to 43% percent.

Among the problems left for future work are the study of the trade-off between reliability and latency under the decoupled association and the investigation of an optimization framework where the optimal association and offloading decisions are made per each MU as well as understanding the effects of other parameters, e.g., UL and DL bandwidth, on the performance of the decoupled access in MEC systems.

REFERENCES

- [1] M. Satyanarayanan, P. Bahl, R. Caceres, and N. Davies, “The case for VM-based cloudlets in mobile computing,” *IEEE Pervasive Comput.*, vol. 8, no. 4, pp. 14–23, Oct. 2009.

- [2] A. Al-Shuwaili, O. Simeone, A. Bagheri, and G. Scutari, "Joint uplink/downlink optimization for backhaul-limited mobile cloud computing with user scheduling," *IEEE Transactions on Signal and Information Processing over Networks*, vol. 3, no. 4, pp. 787–802, Dec 2017.
- [3] F. Boccardi, J. Andrews, H. Elshaer, M. Dohler, S. Parkvall, P. Popovski, and S. Singh, "Why to decouple the uplink and downlink in cellular networks and how to do it," *IEEE Communications Magazine*, vol. 54, no. 3, pp. 110–117, March 2016.
- [4] H. Elshaer, F. Boccardi, M. Dohler, and R. Imer, "Downlink and uplink decoupling: A disruptive architectural design for 5G networks," in *Proc. IEEE Global Communications Conference*, pp. 1798–1803, Dec. 2014.
- [5] K. Smiljkovikj, P. Popovski, and L. Gavrilovska, "Analysis of the decoupled access for downlink and uplink in wireless heterogeneous networks," *IEEE Wireless Communications Letters*, vol. 4, no. 2, pp. 173–176, Apr. 2015.
- [6] H. Jo, Y. J. Sang, P. Xia, and J. G. Andrews, "Heterogeneous cellular networks with flexible cell association: A comprehensive downlink sinr analysis," *IEEE Transactions on Wireless Communications*, vol. 11, no. 10, pp. 3484–3495, Oct. 2012.
- [7] J. G. Andrews, A. K. Gupta, and H. S. Dhillon, "A primer on cellular network analysis using stochastic geometry," *CoRR*, vol. abs/1604.03183, 2016. [Online]. Available: <http://arxiv.org/abs/1604.03183>
- [8] A. Okabe, B. Boots, and K. Sugihara, *Spatial Tessellations: Concepts and Applications of Voronoi Diagrams*. New York, NY, USA: John Wiley & Sons, Inc., 1992.
- [9] Intel, "Intel Xeon W-2125 processor," Sep. 2018. On-line: <https://ark.intel.com/products/126708/>.
- [10] ——, "Intel Xeon processor," Sep. 2018. On-line: <https://ark.intel.com/products/27088/>.
- [11] Qualcomm, "Bandwidth support in LTE standard," Jul. 2012. On-line: <https://transition.fcc.gov/bureaus/oet/tac/tacdocs/meeting71612/PANEL2.3-Gaal-Qualcomm.pdf>.
- [12] A. Miettinen *et al.*, "Energy efficiency of mobile clients in cloud computing," in *Proc. USENIX*, Boston, MA, USA, pp. 4-11, Jun. 2010.